

β -delayed spectroscopy of $^{80}\text{Ge}_{48}$

R. Li^{1,2,*}, D. Verney¹, I. Matea,¹ M. N. Harakeh³, C. Delafosse^{1,4}, F. Didierjean⁵, S. Ebata,⁶ L. A. Ayoubi^{1,4}, H. Al Falou,⁷ G. Benzoni,⁸ F. Le Blanc¹, V. Bozkurt⁹, M. Ciemała,¹⁰ I. Deloncle¹⁰, M. Fallot,¹¹ C. Gaulard,¹ A. Gottardo,¹² V. Guadilla,^{11,†} J. Guillot¹, K. Hadyńska-Klęk,¹³ F. Ibrahim,¹ N. Jovancevic,^{1,‡} A. Kankainen⁴, M. Lebois,¹ T. Martínez¹⁴, P. Napiorkowski¹⁵, B. Roussiere,¹ Yu. G. Sobolev¹⁶, I. Stefan¹⁰, S. Stukalov¹⁶, D. Thisse,¹ and G. Tocabens¹

¹Université Paris-Saclay, CNRS/IN2P3, IJCLab, 91405 Orsay, France

²KU Leuven, Instituut voor Kern- en Stralingsphysica, Celestijnenlaan 200D, B-3001 Leuven, Belgium

³ESRIG, University of Groningen, Zernikelaan 25, 9747 AA Groningen, The Netherlands

⁴Department of Physics, Accelerator Laboratory, P.O. Box 35, University of Jyväskylä, FI-40014 Finland

⁵Institut Pluridisciplinaire Hubert Curien, CNRS/IN2P3 and Université de Strasbourg, Strasbourg, France

⁶Graduate School of Science and Engineering, Saitama University, Saitama, Japan

⁷Faculty of Sciences 3, Lebanese University, Michel Slayman Tripoli Campus, Ras Maska 1352, Lebanon

⁸INFN, Sezione di Milano, Dipartamento di Fisica, Milano, Italy

⁹Nigde University, Science Faculty, Department of Physics, Nigde, Turkey

¹⁰Institute of Nuclear Physics, Polish Academy of Sciences, Krakow, Poland

¹¹Subatech, CNRS/IN2P3, Nantes, EMN, F-44307, Nantes, France

¹²Laboratori Nazionali di Legnaro, I-35020 Legnaro, Italy

¹³Department of Physics, University of Oslo, Oslo, Norway

¹⁴Centro de Investigaciones Energéticas Medioambientales y Tecnológicas (CIEMAT), Madrid, Spain

¹⁵Heavy Ion Laboratory, University of Warsaw, 02-093 Warsaw, Poland

¹⁶Joint Institute for Nuclear Research, Dubna, Russia

(Dated: April 4, 2025)

The β -delayed spectroscopy of ^{80}Ge has been studied using sources of ground and low-lying isomeric states of ^{80}Ga . A hybrid γ -ray spectrometer was used, composed of HPGe detectors for low-energy γ rays detection and phoswich detectors from PARIS array for high-energy γ rays and a plastic detector for β tagging. The new decay level schemes are presented with 19 and 30 states β populated by ^{80g}Ga and ^{80m}Ga , respectively, being reported for the first time. We compare new data with shell-model calculations, and investigate the collective motion in ^{80}Ge via analyzing collectivity evolution in $N = 48$ isotonic and $Z = 32$ isotopic chains.

PACS numbers:

INTRODUCTION

β decay of exotic nuclei provides opportunities to deeply understand the weak interactions in the nuclear medium and to study the structure of daughter nuclei. ^{80}Ga decaying to ^{80}Ge , a nucleus with 32 protons and 48 neutrons, i.e., two-neutron holes in the $N = 50$ closed shell, has several unique characteristics for such studies. First, the ^{80g}Ga and ^{80m}Ga β -decaying states having spin-parity 6^- and 3^- , respectively, can populate a large spin-range from 0 to 8 of daughter states in the nucleus ^{80}Ge , given allowed and first-forbidden transitions. Second, from the energy-window side, the neutron-rich nucleus ^{80}Ga has a very large Q_β value of $10.312(4)$ MeV [1] due to a high isospin asymmetry of 0.23. Third, the structure of ^{80}Ge is considered to be dominated by strong shell effects [2]. However, quadrupole and octupole deformations have also been proposed [3]. Therefore, β decay of ^{80}Ga allows to investigate the impacts of nuclear shell structure and collectivity on β de-

cay particularly in the closed-shell region [4] and to probe the structure of ^{80}Ge such as the pygmy dipole resonance (PDR) [5].

The first β decay study of ^{80}Ga was performed by Hoff et al. through neutron-induced fission of ^{235}U , and the level scheme was determined up to 6.155 MeV. The energy region from 6.155 MeV to Q_β value is blank. The cumulated I_β intensity is 73.94%. Compared with $\% \beta^- \gamma = 99.14$, twenty-five percent branching-ratios were not observed [6]. Following the observation of a low-lying 22.4 keV isomeric state in ^{80}Ga [7], Verney et al. separated the decay level schemes of the ground state and isomeric state but only up to 3.5 MeV [3]. Recently, β decay of a mixed source $^{80g+m}\text{Ga}$ was performed using proton-induced fission with thick UC_x target. However, this measurement suffered from serious contamination of ^{80}Rb of 78% [8]. The latest study took advantage of ^{80m}Ga only [9].

In this article, we disentangle the decay level schemes fed by the two β -decaying states of ^{80}Ga in the whole Q_β window. Separated decay level schemes up to S_n are established. New data are compared with shell-model calculations. The collective motion in ^{80}Ge is studied via systematic analysis of collectivity evolution in $N = 48$ isotonic and $Z = 32$ isotopic chains.

EXPERIMENT

The measurement was performed at the Accélérateur Linéaire et Tandem à Orsay (ALTO) ISOL facility [10]. A radioactive low-energy ^{80}Ga ion beam was produced by the photofission of a UC_x target induced by a 50-MeV electron beam with an intensity of $\sim 7 \mu\text{A}$. For beam purification, the laser ionized Ga beam was mass selected. Since at around $A=80$ the only surface ionized component of a photofission generated ion beam is Ga, complete isotope purity was achieved, with zero ^{80}Rb contamination. This cleanliness was tested by the β -gated γ spectrum. No contaminated γ -rays, like β^+/ϵ -delayed 616.7 keV γ -line of ^{80}Kr , were found in the spectrum. Only γ -rays from ^{80}Ge and its daughter and granddaughter nuclei were observed. Then, a ^{80}Ga beam with yield of $\sim 10^4$ pps was directed and collected by the tape system of the BEDO (BEta Decay studies at Orsay) setup, which was moved periodically for minimizing the daughters activity [11]. The time settings were 0.5 s for background, 5 s for ion collection and 5 s for decay measurement.

The emitted radiations were detected by a hybrid array around the collection spot. It consisted of one cylindrical plastic scintillator for β tagging, surrounded by two high-purity germanium detectors (HPGe), one clover HPGe and one coaxial HPGe, and three PARIS clusters [12, 13]. Each cluster comprises 9 optically isolated segmented phoswiches. A phoswich is composed of two layers of different scintillators and a photomultiplier. The first layer is a 2 inch \times 2 inch \times 2 inch Lanthanum Bromide crystal (LaBr_3), one of the three clusters is Cerium Bromide (CeBr_3). The second layer is a 2 inch \times 2 inch \times 6 inch Sodium Iodide (NaI) crystal. The high energy resolution of the HPGe working in the 0 - 6 MeV energy range makes very effective the γ - γ coincidence technique not only to reconstruct the transition cascades but also to suppress the background drastically. PARIS working in the 6 - 10 MeV energy range has high detection efficiency. The detectors were energy calibrated up to 9 MeV using sources including $^{58}\text{Ni}(\text{n-th},\gamma)$ with energy of 8999.267(15) keV. The energy resolution of HPGe detectors is 2.541 keV at 1109 keV (a γ -line of ^{80}Ge) from summed spectrum. Considering 10.39(2), 12.65(5), 1.65(2) and 2.78(4) ns time resolutions of coaxial HPGe, clover HPGe, $\text{LaBr}_3(\text{Ce})$ and NaI, respectively, 50 ns was chose as the γ - γ coincidence time window. The detection efficiency of HPGe detectors including one clover HPGe and one coaxial HPGe is 3.134(5)% at 1085.836 keV. The energy resolution and detection efficiency of PARIS clusters are 112

keV and 0.30(2)%, respectively, at 7.18 MeV, under mode 3; signals only come from $\text{LaBr}_3(\text{Ce})$ crystals and are vetoed by outer-layer NaI detectors, but the energy is added back within 27 phoswich detectors. Data were acquired in a triggerless mode.

For extracting precise $\log ft$ and $B(\text{GT})$ values, counting precursors with high precision is critical. The applied methodology was handling the Bateman equations using the total β spectrum. This allows one to determine the activity of the precursors and the intensity of the radioactive beam. The final counts of precursor ^{80}Ga are: $N_{^{80}\text{Ga}}^{\text{decayed}} = 1.41(8) \times 10^8$, $N_{^{80}\text{Ga}}^{\text{decayed}} = 2.40(8) \times 10^8$. The uncertainties on these numbers originate from the uncertainties of input parameters including half-lives of precursor and daughter and granddaughter nuclei, P_n and the detection efficiency of β detector.

In order to obtain two separated decay level schemes of ^{80}gGa and ^{80m}Ga , it is essential to identify the β feeding precursor for each state of the daughter nucleus. For the identification methods, we refer to Refs. [3, 4].

EXPERIMENTAL RESULTS

The β -gated γ spectra measured during the experiment are presented in Figs. 1. One can observe the β -delayed γ -rays belonging to daughter and granddaughter nuclei ^{80}Ge , ^{80}As and ^{80}Se with different marks. In addition, γ -ray deexcitation of the nucleus ^{79}Ge , populated through β -delayed neutron emission of ^{80}Ga , is also detected. No other γ -rays were observed in the spectra, which proves the beam purity. All these γ -rays populated through deexcitation of the excited states of ^{80}Ge allowed us to improve and enrich the decay level scheme of ^{80}Ge . In the present work, a total of 112 characteristic half-lives of activities of β -delayed γ rays could be determined; see tabulated γ information in Tab. 1 in Ref. [4]. Among them 70 were assigned to the decay of ^{80}gGa and 65 to the decay of ^{80m}Ga . Twenty-three γ -rays are emitted by both isomers. Among the 70 γ -rays, 29 γ -rays are observed for the first time, indicated by the red color lines in the decay level scheme in Figs. 2 and 3. Among the 65 γ -rays, 35 γ -rays are detected and reported for the first time.

For the precursor identification, only ten states out of a total of 77 populated states were assigned to β feedings from both ^{80}gGa and ^{80m}Ga simultaneously. They are the levels with the energies of 1972.2, 3423.4, 3515.5, 3610.7, 3721.1, 3752.2, 4029.3, 4408.2, 4462.5, and 5806.3 keV. The summed I_β of these ten states are 8.1(6)% and 13.9(8)% in the decay level schemes of ^{80}gGa and ^{80m}Ga , respectively. The γ -lines from these states are assigned to 50% from ^{80}gGa and 50% from ^{80m}Ga . It is worth pointing out that having the intensity distributed in both level schemes for some γ rays and levels can introduce a systematic error in the feedings. Further checks of these ten states with high statistics deserve being pursued in future experiments.

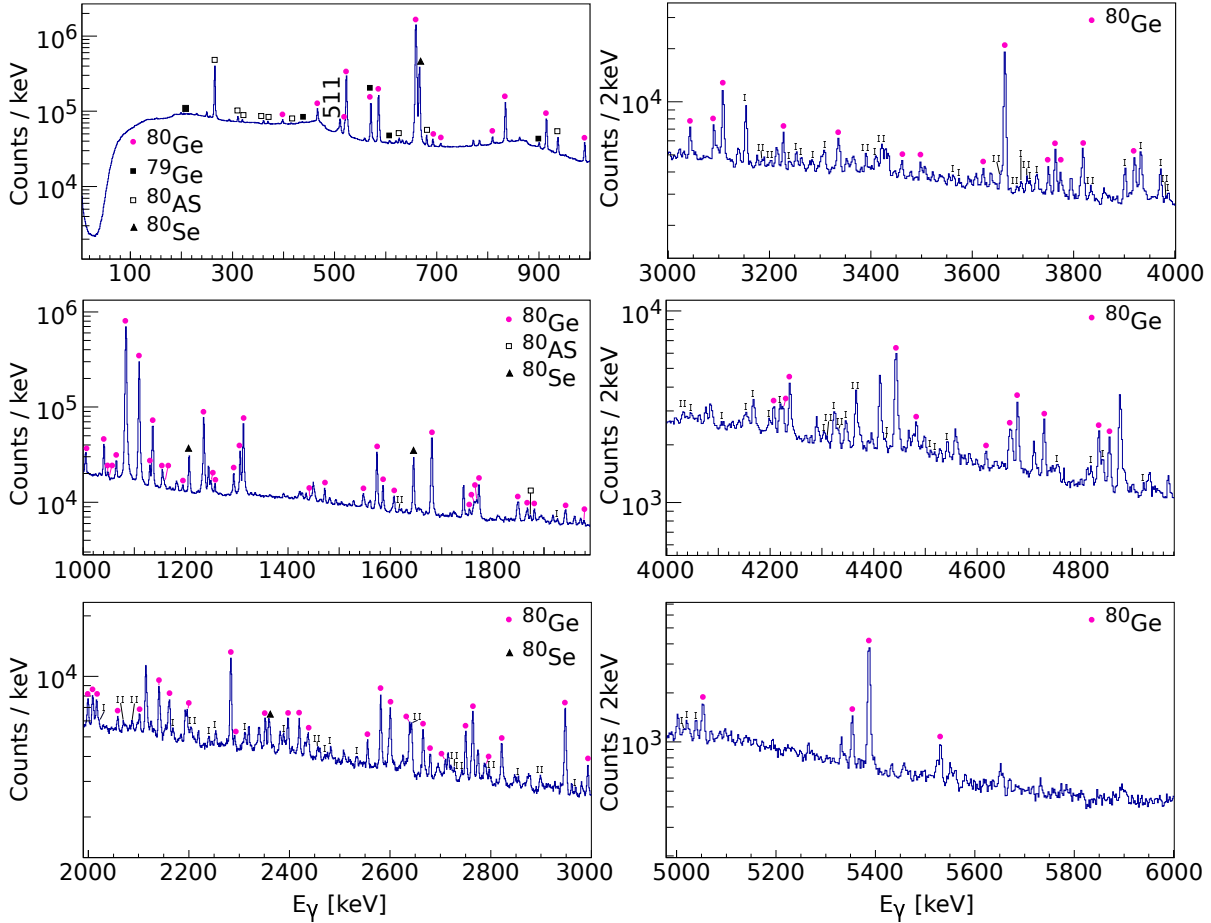


FIG. 1: β -gated γ spectra in the range 0 to 6000 keV. The marked lines are attributed to transitions in daughter nuclei: filled circles = ^{80}Ge ; filled squares = ^{79}Ge ; empty squares = ^{80}As and filled triangles = ^{80}Se . I and II symbols denote single- and double-escape peaks, respectively. Note that I and II are not subsequent.

From the present data, one can place 45 excited states of ^{80}Ge populated in the β decay of ^{80g}Ga as shown in Figs. 2 and 3. Nineteen states are reported for the first time. The scheme was built based on the β - γ - γ coincidence relationships. The excitation energies of states were obtained through calculating the weighted average value of distinct deexcitation cascades. For example, the excitation energy for the state at 5801.1(7) keV was obtained by considering the three following deexcitation cascades: 2948.2(5) + 2852.3(5) keV, 2821.9(5) + 2978.5(5) keV and 2115.0(4) + 3686.9(6) keV. The weight is according to the strength (I_γ^{rel}) of the three γ -rays 2948(5) keV, 2821.9(5) keV and 2115.0(4) keV. They are 2.42(9)%, 1.01(6)% and 2.39(9)% individually. Then, a weighted energy level of 5801.1 keV state is obtained. The uncertainty 0.7 keV is also a weighted result of the three cascades.

The I_β values were calculated using the balance of the observed feeding and depopulating γ activities, which means that for a given state, the β feeding is the difference between the γ -feeding to and γ -decay from this state. Since the cumulated values of I_β from ^{80g}Ga and ^{80m}Ga reach 79.1(25)% and

85.3(36)%, respectively, one can conclude that some states are unobserved in this work especially in the high energy around S_n (8.08 MeV) region. These states would deexcite to some low-lying states like 1742.9, 2266.0, 2852.3, 2978.5, 3423.4, 3445.3, 3515.5, 3686.9, 3988.3 and 4026.2 keV. In order to avoid being over-weighted, the I_β of these states were just given an upper limit in this work.

The log ft value calculations were performed using the NNDC online procedure [14], wherein, the $T_{1/2}$, E_{energy} and I_β were from this work and the used Q_β was taken from Ref. [1].

As presented in Figs. 4 and 5, 48 of excited states of ^{80}Ge were populated by ^{80m}Ga β decay and 30 of these states are proposed for the first time with red colors in current work. Of the 30 new states, 23 are located interestingly above 4 MeV. This means the I_β of low-lying states were over-weighted in previous work while down-weighted in the high-energy region. It was caused by the missing of unobserved high-energy γ -rays. The states at 7840(71) keV and 7996(72) keV were determined based on the observation of high-energy γ -rays,

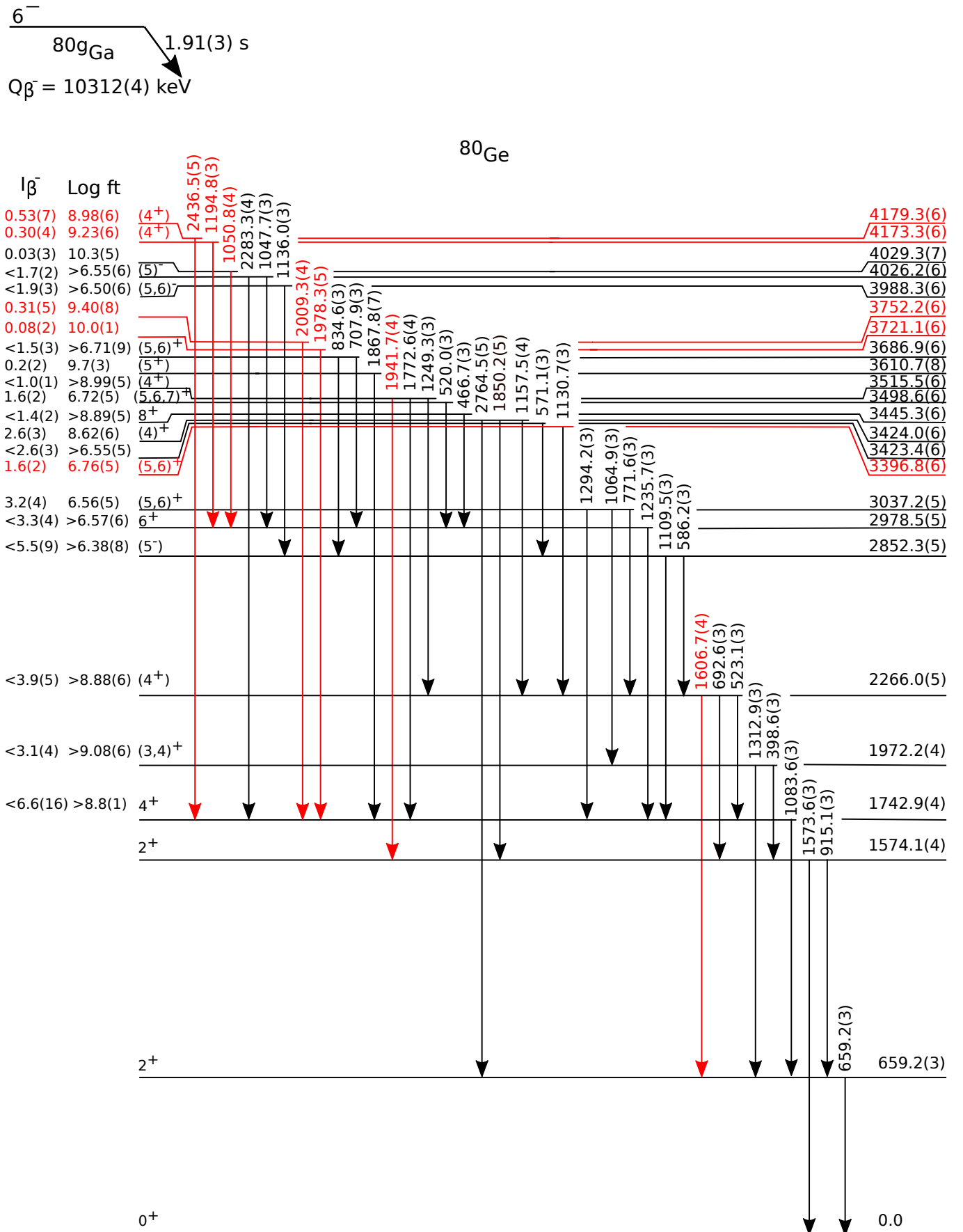


FIG. 2: Level scheme of ^{80}Ge up to 4.2 MeV in excitation energy populated following the β decay of ^{80}gGa . For the sake of clarity, the decay scheme has been split in two sections with the one for the higher energies plotted in Fig. 3.

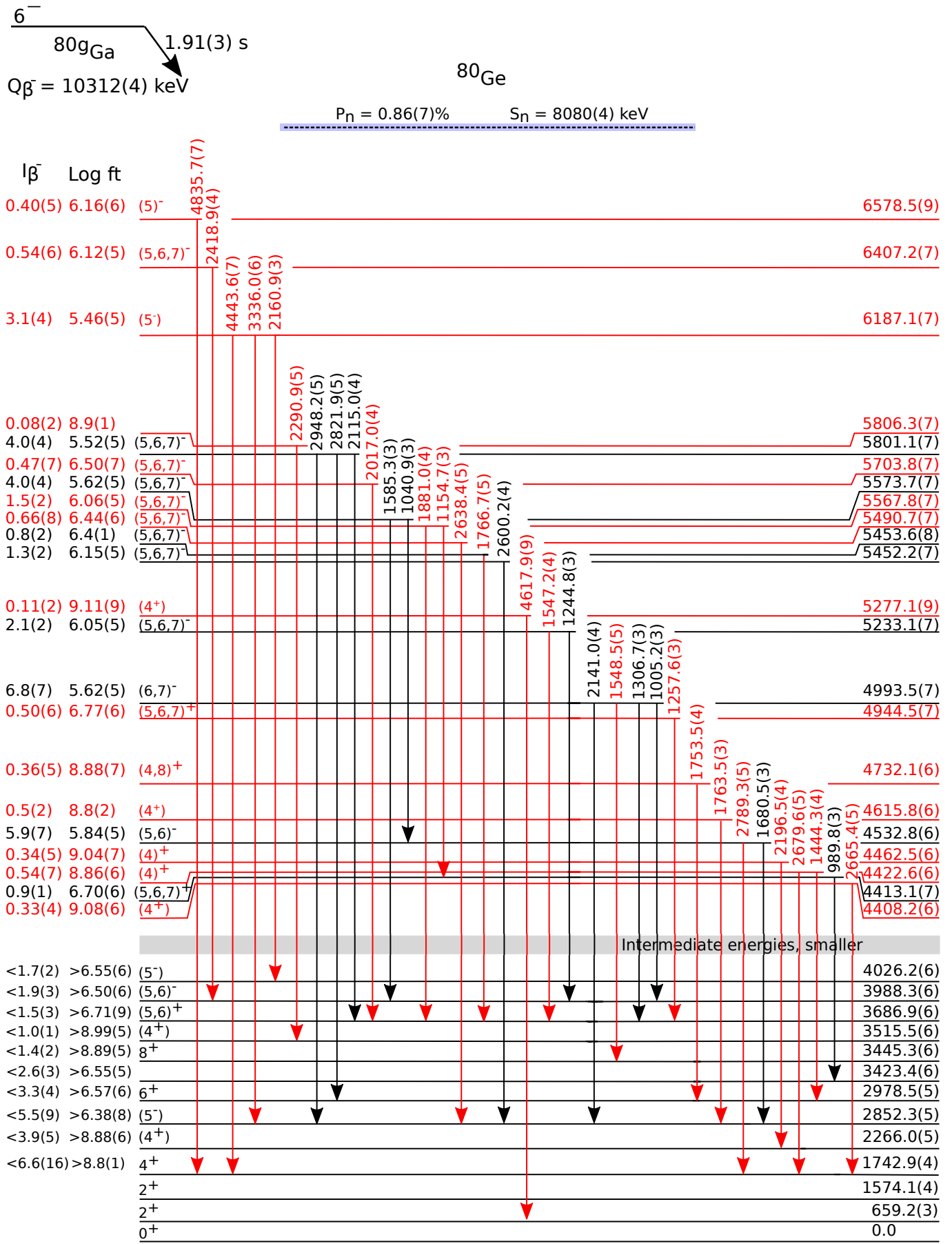


FIG. 3: Level scheme of ⁸⁰Ge populated following the β decay of ^{80g}Ga containing the high-lying states between 4.2 and 8 MeV in excitation energy.

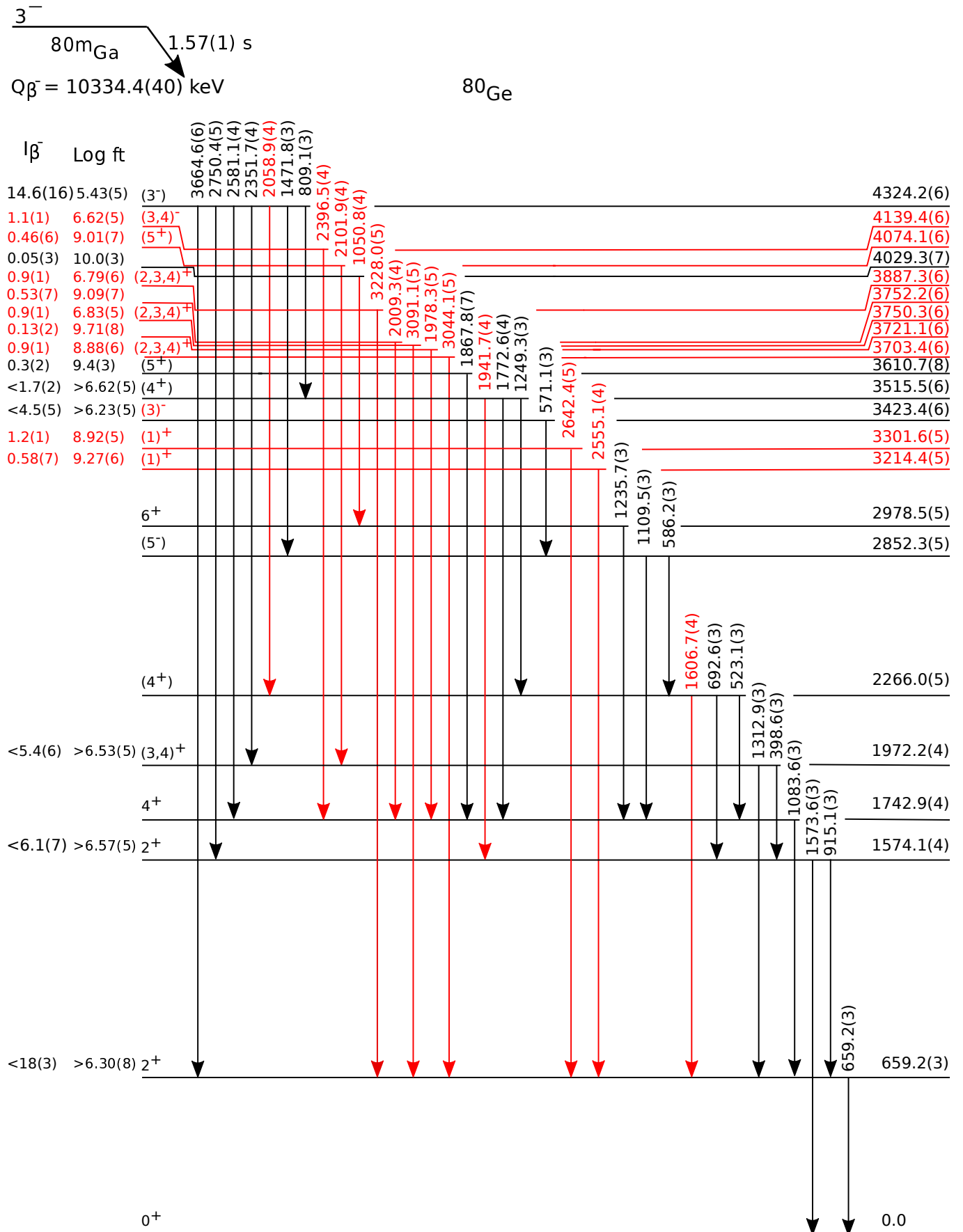


FIG. 4: Level scheme of ^{80}Ge up to 4.4 MeV in excitation energy populated following the β decay of ^{80m}Ga . For the sake of clarity, the decay scheme has been split in two sections with the one for the higher energies plotted in Fig. 5.

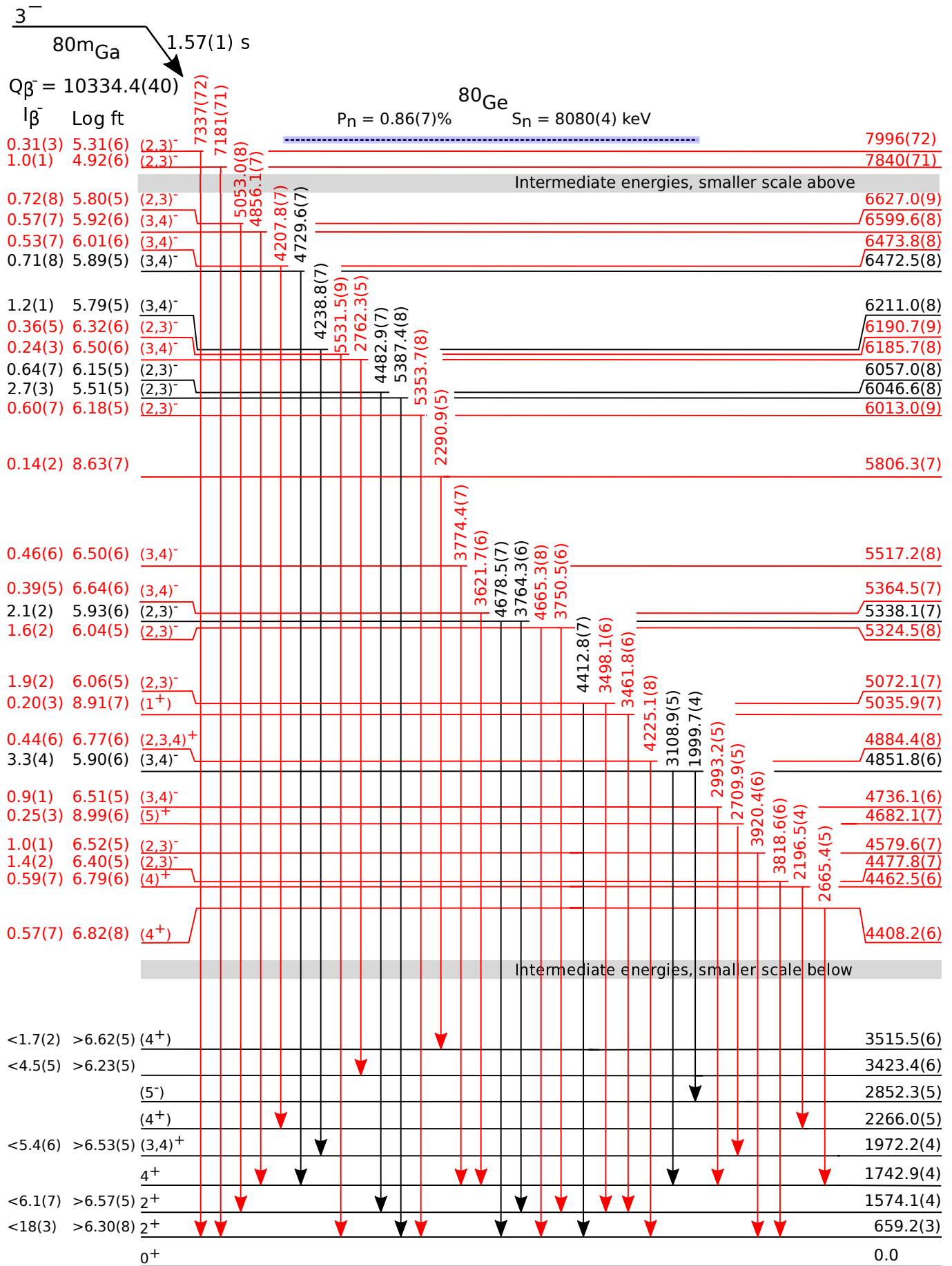


FIG. 5: Level scheme of ⁸⁰Ge populated following the β decay of ^{80m}Ga containing the high-lying states between 4.4 and 8 MeV in excitation energy.

7181(71) keV and 7337(72), by PARIS array. The I_β , $\log ft$ and their uncertainty analysis procedures are the same as aforementioned. It is worth noting that the Q_β for ^{80m}Ga is 10334.4(40) keV with including 22.4 keV [1] corresponding with the excitation energy of the isomeric state. The spin-parity assignment will be discussed in the next section.

DISCUSSION

Log ft values are ones of the most important observables in the β decay study, which are affected by the nuclear structure of the parent and daughter nuclei. It is also vital experimental data that can be used to support the theory development. We systematically analyzed the $\log ft$ values of $N = 49$ isotones, see Tab. 5.5 in Ref. [15]. It provides a reference to determine the types of β transitions. Along with the proton number increasing the $\log ft$ values of allowed and First-Forbidden (FF) transitions also increase. It means that in $N = 49$ isotonic chain from exotic to stable nuclei the allowed and FF β decay probabilities decrease, which keeps good agreement with nuclear characteristics.

In this neutron-rich region, it is often difficult to separate allowed from FF transitions since the latter becomes significant for neutron-rich nuclei. The references for the identification of β transition type are global statistics for the whole nuclear chart and the local standard. In the former [16, 17], $\log ft$ value is 3-4 for super-allowed β decay, 4-8 for allowed transition, 6-9 for FF transition, 8-11 for first-forbidden unique (1U) transition. Since the 0_1^+ , 2_1^+ , 4_1^+ , 6_1^+ and 8_1^+ levels are well identified in ^{80}Ge , the transitions $6^-(^{80}\text{Ga}) \rightarrow 4_1^+$, $6^-(^{80}\text{Ga}) \rightarrow 6_1^+$ and $6^-(^{80}\text{Ga}) \rightarrow 8_1^+$ can provide a local reference of FF and 1U transitions. Likewise, $3^-(^{80m}\text{Ga}) \rightarrow 2_1^+$ and $3^-(^{80m}\text{Ga}) \rightarrow 2_2^+$ provide references for FF transition as well.

Based on this analysis, among the β transitions of ^{80}Ga , the allowed transition character was assigned if the " $\log ft < 6.6$ ", which populated $(5,6,7)^-$ states; FF transition was assigned if " $\log ft > 6.6$ and $\log ft < 6.8$ ", which populated $(5,6,7)^+$ states; 1U transition was assigned if " $\log ft > 6.8$ " and the $\log ft$ value was calculated again using 1U formula, which populated $(4,8)^+$. For ^{80m}Ga , the same identifying standards were adopted. Therefore, allowed transitions populated $(2,3,4)^-$ states; FF transitions populated $(2,3,4)^+$ states; 1U transitions populated $(1,5)^+$ states. This analysis is based on the hypothesis that the spin-parity of $^{80g+m}\text{Ga}$ (6^- and 3^-) are correct [7], and that the second forbidden transition with " $\log ft > 11$ " in the global statistics [16, 17] was negligible. Combined with this β transition identification, the candidate spin-parity of states of ^{80}Ge were given on the prior consideration of E1, E2 and M1 multipolarities of γ deexcitations.

The final results are presented in Tables I and II. A total number 43 of β decays from the 6^- state was determined and 44 from the 3^- state. The existence of unobserved γ -rays, for low-lying states, could significantly decrease the deduced β feedings and consequently increase the $\log ft$ values. There-

fore, the $\log ft$ values of low-lying states in $^{80g+m}\text{Ga}$ decay level schemes were just provided as minimum values, which guarantees that the branching ratios of low-lying states are not over-weighted. Besides I_β , $\log ft$ and J^π information, the "X" value of each state was also presented in the tables.

TABLE I: Excited states of ^{80}Ge β fed by ^{80g}Ga .

E_{state} (keV)	I_β	$\log ft$	J^π	"X"
1742.9 4	<6.6 16	>8.8 1	4^+	0.1 14
1972.9 4	<3.1 4	>9.08 6	$(3,4)^+$	0.60 32
2266.0 5	<3.9 5	>8.88 6	(4^+)	0.33 95
2852.3 5	<5.5 9	>6.38 8	(5^-)	-0.2 12
2978.5 5	<3.3 4	>6.57 6	6^+	-0.37 34
3037.2 5	3.2 4	6.56 5	$(5,6)^+$	0.25 16
3396.8 6	1.6 2	6.76 5	$(5,6)^+$	0.31 25
3423.4 6	<2.6 3	>6.55 5		0.56 32
3424.0 6	2.6 3	8.62 6	(4^+)	0.40 31
3445.3 6	<1.4 2	>8.89 5	8^+	0.10 34
3498.6 6	1.6 2	6.72 5	$(5,6,7)^+$	0.17 24
3515.5 6	<1.0 1	8.99 5	(4^+)	0.55 42
3610.7 8	0.2 2	9.7 3	(5^+)	0.5 59
3686.9 6	<1.5 3	>6.71 9	$(5,6)^+$	-0.7 17
3721.1 6	0.08 2	10.0 1		0.5 14
3752.2 6	0.31 5	9.40 8		0.42 70
3988.3 6	<1.9 3	>6.50 6	$(5,6)^-$	-0.33 74
4026.2 6	<1.7 2	>6.55 6	(5^-)	0.16 66
4029.3 7	0.03 3	10.3 5		0.4 59
4173.3 6	0.30 4	9.23 6	(4^+)	0.32 75
4179.3 6	0.53 7	8.98 6	(4^+)	0.22 67
4408.2 6	0.33 4	9.08 6	(4^+)	0.54 44
4413.1 7	0.9 1	6.70 6	$(5,6,7)^+$	0.05 89
4422.6 6	0.54 7	8.86 6	(4^+)	0.14 54
4462.5 6	0.34 5	9.04 7	(4^+)	0.49 63
4532.8 6	5.9 7	5.84 5	$(5,6)^-$	0.02 22
4615.8 6	0.5 2	8.8 2	(4^+)	0.3 41
4732.1 6	0.36 5	8.88 7	$(4,8)^+$	0.25 67
4944.5 7	0.50 6	6.77 6	$(5,6,7)^+$	0.24 42
4993.5 7	6.8 7	5.62 5	$(6,7)^-$	0.12 14
5233.1 7	2.1 2	6.05 5	$(5,6,7)^-$	0.18 20
5277.1 9	0.11 2	9.11 9	(4^+)	-0.1 20
5452.2 7	1.3 2	6.15 5	$(5,6,7)^-$	0.18 25
5453.6 8	0.8 2	6.4 1	$(5,6,7)^-$	0.1 26
5490.7 7	0.66 8	6.44 6	$(5,6,7)^-$	0.19 48
5567.8 7	1.5 2	6.06 5	$(5,6,7)^-$	0.20 39
5573.7 7	4.0 4	5.62 5	$(5,6,7)^-$	0.11 15
5703.8 7	0.47 7	6.50 7	$(5,6,7)^-$	0.24 95
5801.1 7	4.0 4	5.52 5	$(5,6,7)^-$	0.22 13
5806.3 7	0.08 2	8.9 1		0.6 12
6187.1 7	3.1 4	5.46 5	(5^-)	0.13 32
6407.2 7	0.54 6	6.12 5	$(5,6,7)^-$	0.01 45
6578.5 9	0.40 5	6.16 6	(5^-)	-0.16 71

The spin-parity of states populated by β transitions with reduced $\log ft$ values less than 6.0, can be adopted with high confidence. In other words, these transitions can be assigned to Gamow-Teller transitions. For the states with β transition $\log ft$ value between 6 to 6.6, their spin-parity assignments are regarded as tentative due to the serious competition between allowed and FF β transitions. Furthermore, Fermi decay would populate 3^- and 6^- states in ^{80}Ge , but such transitions only happen with low $\log ft$ values to isobaric analog states (IAS) which are located at much higher energy than levels observed in this study. In addition, isospin mixing in the low-lying states (below $S_n = 8.08$ MeV) is expected to be ex-

TABLE II: Excited states of ^{80}Ge β fed by ^{80m}Ga .

E_{state} (keV)	I_{β}	$\log ft$	J^{π}	"X"
659.2 3	<18 3	>6.30 8	2^+	1.0 20
1574.1 4	<6.1 7	>6.57 5	2^+	0.83 27
1972.2 4	<5.4 6	>6.53 5	$(3,4)^+$	0.60 32
3214.4 5	0.58 7	9.27 6	$(1)^+$	0.82 72
3301.6 5	1.2 1	8.92 5	$(1)^+$	0.46 30
3423.4 6	<4.5 5	>6.23 5	$(3)^-$	0.56 32
3515.5 6	<1.7 2	>6.62 5	(4^+)	0.55 42
3610.7 8	0.3 2	9.4 3	(5^+)	0.5 59
3703.4 6	0.9 1	8.88 6	$(2,3,4)^+$	0.83 69
3721.1 6	0.13 2	9.71 8		0.5 14
3750.3 6	0.9 1	6.83 5	$(2,3,4)^+$	0.65 55
3752.2 6	0.53 7	9.09 7		0.42 70
3887.3 6	0.9 1	6.79 6	$(2,3,4)^+$	0.77 65
4029.3 7	0.05 3	10.0 3		0.4 59
4074.1 6	0.46 6	9.01 7	(5^+)	1.3 12
4139.4 6	1.1 1	6.62 5	$(3,4)^-$	0.67 57
4324.2 6	14.6 16	5.43 5	(3^-)	0.72 12
4408.2 6	0.57 7	6.82 8	(4^+)	0.54 44
4462.5 6	0.59 7	6.79 6	$(4)^+$	0.49 63
4477.8 7	1.4 2	6.40 5	$(2,3)^-$	0.85 74
4579.6 7	1.0 1	6.52 5	$(2,3)^-$	1.17 67
4682.1 7	0.25 3	8.99 6	(5^+)	0.8 18
4736.1 6	0.9 1	6.51 5	$(3,4)^-$	0.65 61
4851.8 6	3.3 4	5.90 6	$(3,4)^-$	0.60 22
4884.4 8	0.44 6	6.77 6	$(2,3,4)^+$	1.2 19
5035.9 7	0.20 3	8.91 7	(1^+)	1.2 22
5072.1 7	1.9 2	6.06 5	$(2,3)^-$	0.84 41
5324.5 8	1.6 2	6.04 5	$(2,3)^-$	0.76 58
5338.1 7	2.1 2	5.93 6	$(2,3)^-$	0.60 46
5364.5 7	0.39 5	6.64 6	$(3,4)^-$	0.88 14
5517.2 8	0.46 6	6.50 6	$(3,4)^-$	1.2 17
5806.3 7	0.14 2	8.63 7		0.6 12
6013.0 9	0.60 7	6.18 5	$(2,3)^-$	1.22 84
6046.6 8	2.7 3	5.51 5	$(2,3)^-$	1.19 32
6057.0 8	0.64 7	6.15 5	$(2,3)^-$	0.59 58
6185.7 8	0.24 3	6.50 6	$(3,4)^-$	0.7 16
6190.7 9	0.36 5	6.32 6	$(2,3)^-$	0.7 13
6211.0 8	1.2 1	5.79 5	$(3,4)^-$	1.02 64
6472.5 8	0.71 8	5.89 5	$(3,4)^-$	1.45 85
6473.8 8	0.53 7	6.01 6	$(3,4)^-$	0.7 13
6599.6 8	0.57 7	5.92 6	$(3,4)^-$	0.80 67
6627.0 9	0.72 8	5.80 5	$(2,3)^-$	0.78 79
7840.71	1.0 1	4.92 6	$(2,3)^-$	0.83 33
7996.72	0.31 3	5.31 6	$(2,3)^-$	1.24 56

tremely small, which is reflected in the $\log ft$ values as one can find that there is no state which has a $\log ft$ value of ~ 3.5 .

The shell-model (SM) calculation is performed with the core of $N=50$ and $Z=28$, using two-hole and four-particle states for neutrons and protons, respectively. The pairing plus quadrupole-quadrupole interaction is applied to the SM calculation. Its detail is written in Ref. [18]. Fig. 6 presents the theoretical results. For comparison, experimentally observed states populated by β decay of $^{80g+m}\text{Ga}$ are inserted in the figure: two columns with filled circles. Red and blue colors represent positive- and negative-parity, respectively, consistent with colors used in plotting theoretical data. Note that their spins are listed in Tables I and II instead of the values given on the x-axis. Colored regions are β population favored by ^{80m}Ga and ^{80g}Ga in spin dimension given allowed and first-forbidden non-unique (ffnu) transitions. One observes that low-lying

states, e.g., 2_1^+ , 2_2^+ , 4_1^+ , 6_1^+ and 8_1^+ , are reproduced very well. In other words, given these levels can be described by the configuration mixing of valence particle states, their collectivities might be small. However, high-lying states located between 6 MeV and 8 MeV especially with negative-parity can not be reproduced by shell-model. It demonstrates that valence space used in the calculation, made up from nucleons occupying the $g_{9/2}$, $p_{1/2}$, $p_{3/2}$ and $f_{5/2}$ orbitals [18], is not enough for generating high-lying negative-parity states. The $f_{7/2}$ or other orbits in the core should be active in the calculation to describe the experimental data better. It is because considering that the β transition can occur in the deep-bound neutron, the core could be degenerated to ^{56}Ni or even collapses. The levels cannot be described by the shell-model, which indicates we should consider the core excitation or more valence nucleons or the collective motion, such as vibration or rotation.

Fig. 7(a) shows the $E(2_1^+)$ values along the chains of $N = 48$ and $N = 50$ isotones. Both exhibit two local maxima at $Z = 28$ (Ni) and $Z = 40$ (Zr) attributed to spin-orbit coupling (OS) and harmonic oscillator (HO) shell closures, respectively. These assessments are reinforced by their low $B(E2)$ values, implying small quadrupole collectivities. It is due to the double-magic character of $^{28}\text{Ni}_{50}$ and $^{40}\text{Zr}_{50}$ while another double-magic nucleus ^{100}Sn still keeps its mystery. On the contrary, the $E(2_1^+)$ values for ^{80}Ge and ^{82}Se are the lowest of the $N = 48$ isotopic chain. This is an indication for higher collectivity. The fact that the maximum of quadrupole collectivity emerges already at ^{80}Ge in the $N = 48$ isotonic chain, two neutrons away from magic number $N = 50$, justifies the interest in this nucleus for studying the collectivity near the magic number region.

Fig. 7(b) displays the experimental $B(E2)\uparrow (0_1^+ \rightarrow 2_1^+)$ reduced transition probabilities for $N = 48$ and $N = 50$ isotones as functions of proton numbers, between 30 and 42, measured in Coulomb excitation experiments [19]. It sheds light on the behavior of nuclear collectivity in the $N = 48$ and $N = 50$ isotopes between neutron-rich nuclei together with nuclei in the stability valley. One finds that the $B(E2)\uparrow$ value increases from $Z = 30$ to $Z = 34$ and $Z = 32$, then decreases until the minimum at $Z = 40$. Two conclusions can be drawn: first, the quadrupole $E2$ excitations are quenched at closed shells ($Z = 28$ and $Z = 40$) because any excitation has to overcome the large gaps of doubly-magic nuclei; second, on the contrary, the mid-shell nuclei $Z = 32$ (Ge) and $Z = 34$ (Se), which have free levels and valence nucleons for their excitation, exhibit the highest $B(E2)\uparrow$ values among the $N = 48$ and $N = 50$ isotones. This highest collectivity is correlated with larger deformation. In conclusion, from the $B(E2)\uparrow$ curves in the nuclei of this region, ^{80}Ge has a stronger collectivity, which is consistent with the previous $E2$ analysis.

Furthermore, Fig. 7(c) presents the excitation energy of 8_1^+ isomeric states of the $N = 48$ isotonic chain. These 8^+ isomers have been determined to be built on the two neutron-hole configurations $vg_{9/2}^{-2}$ before $Z = 40$. This was determined

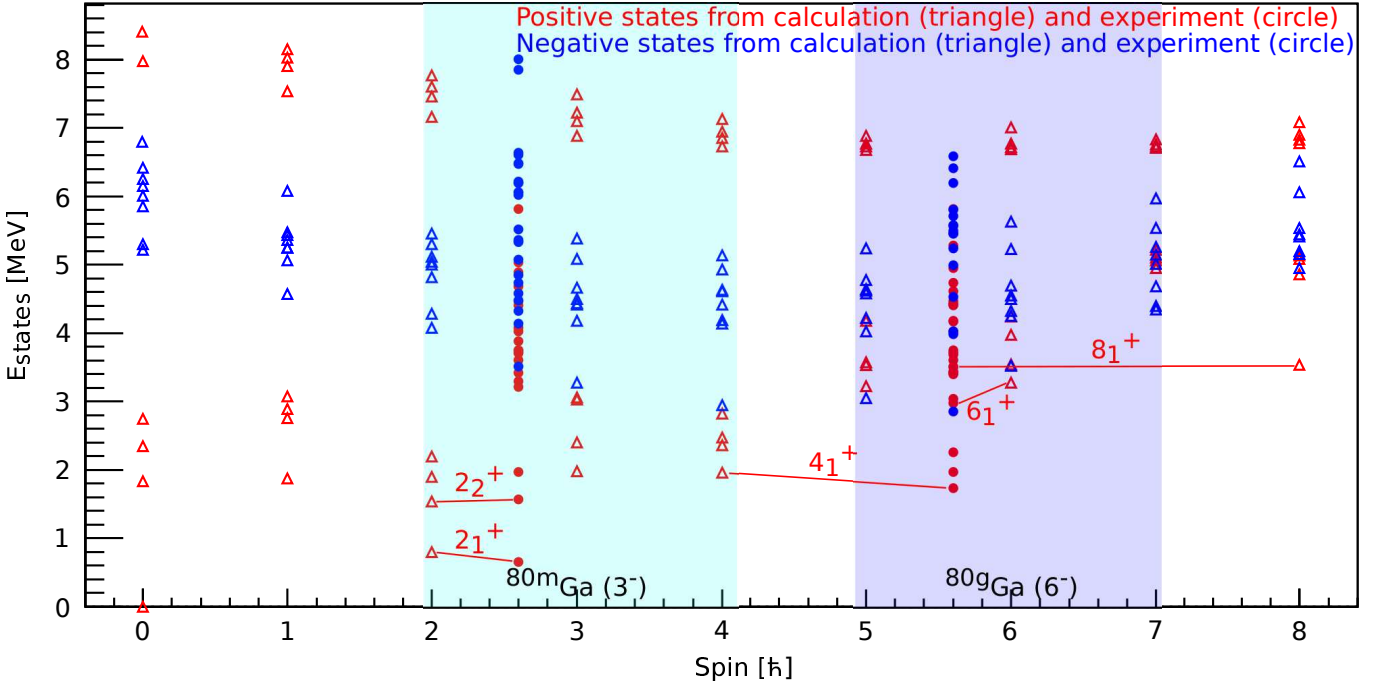


FIG. 6: Comparison between results from experiment and shell-model calculation [18]. Filled blue circles: negative-parity states β populated by ^{80m}Ga (left) and ^{80g}Ga (right), respectively; Filled red circles: experimental positive-parity states; Open blue triangles: negative-parity states from shell-model calculation; Open red triangles: positive-parity states from calculation. Note that the spins of the experimentally observed states are not the values given on the x-axis but are listed in Tables I and II.

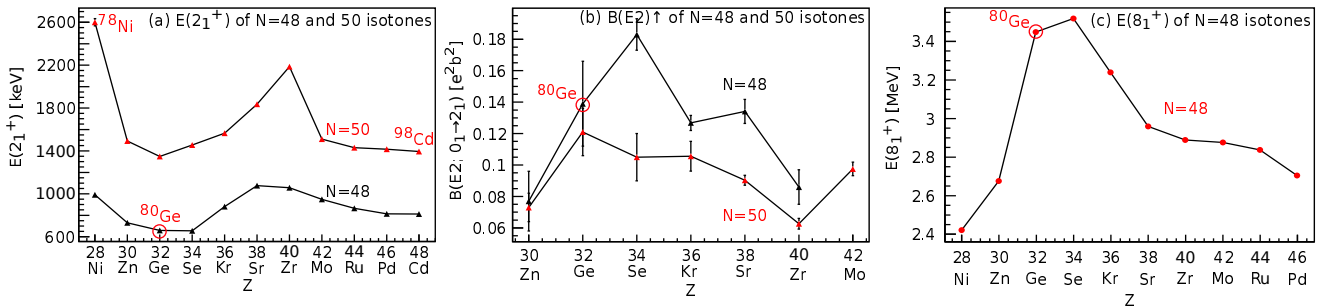


FIG. 7: (a): $E(2_1^+)$ of $N = 48$ and $N = 50$ isotonic chains; (b): $B(E2)^\uparrow$ of $N = 48$ and $N = 50$ isotonic chains; (c): Energy of 8_1^+ states relative to 0_1^+ for the $N = 48$ isotones as a function of the proton number. Data are from ENSDF [19]

thanks to g factor measurement of 8_1^+ states and comparison with the g factor of the $9/2^+$ state, from $^{87,88}\text{Sr}$, $g(8^+[\text{vg}_{9/2}^-]) = g(9/2^+[\text{vg}_{9/2}^-]) = -0.243(4)$ [20]). Therefore, the energy of 8^+ states can reveal the 2-neutron hole potential V_{2h} in the $N = 48$ isotonic chain. ^{80}Ge together with ^{82}Se have the maximum values of 8^+ energy in accordance with largest V_{2h} which is in good agreement with their large collectivities as shown in Fig. 7 (a) and (b).

In order to further investigate the collectivity of ^{80}Ge , an analysis of Ge isotopes was performed. In the nuclear tri-axial deformation research, the even-even Ge isotopes have attracted much attention and many endeavors have been made

to study them including experimental and theoretical work. In $^{72,74,76,78}\text{Ge}$, the γ -bands have been experimentally observed, which provide evidences the triaxialities [21–24]. The $B(E2)^\uparrow$ of Ge isotopes are drawn in Fig. 8. In addition, $B(E2)^\uparrow$ of $\text{Ni}(Z=28)$ and $\text{Zn}(Z=30)$ isotopes are also presented. Moreover, the behavior of the $B(E2)$ function of the Ge isotopes is quite different, when compared with Ni isotopes, as it increases strongly from $N=36$ until $N = 42$. Then, it decreases toward $N=50$. However, ^{80}Ge still possesses a large $B(E2)$ value. Furthermore, Ge isotopes present larger $B(E2)$ values when compared with Ni and Zn isotopes.

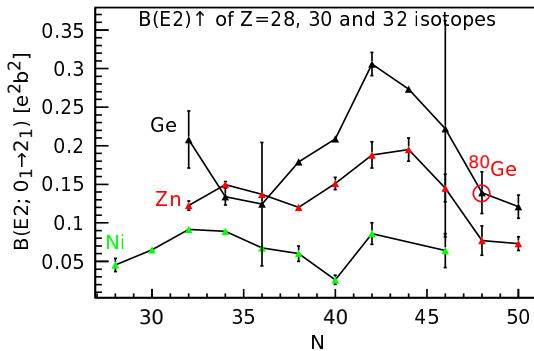


FIG. 8: $B(E2)^\uparrow$ of $Z = 28, 30, 32$ isotopic chains as functions of neutron number. Data are from ENSDF [19].

CONCLUSION

In conclusion, the detailed β -delayed γ spectroscopy of ^{80}Ge has been presented with 19 and 30 states being reported for the first time β populated by ^{80g}Ga and ^{80m}Ga , respectively. New data are compared with shell-model calculations. The collective motion in ^{80}Ge has been studied via analyzing collectivity evolution in $N = 48$ isotonic and $Z = 32$ isotopic chains. For determination of spin-parity of observed states, angular distributions or correlations of deexcitation γ rays deserve being measured in the future.

The authors thankfully acknowledge the work of the ALTO technical staff for the excellent operation of the ISOL source. Prof. N. Yoshinaga supplies the shell model calculation data. R. Li acknowledges supports by China Scholarship Council under Grant No.201804910509 and by a KU Leuven post-doctoral scholarship. C. Delafosse, A. Kankainen and L. A. Ayoubi have received funding from European Union's Horizon 2020 research and innovation program under grant agreement NO. 771036 (ERC CoG MAIDEN). Use of PARIS modular array from PARIS collaboration and Ge detectors from the French-UK IN2P3-STFC Gamma Loan Pool are acknowledged.

M. Cheikh Mhamed, E. Cottreau, P. V. Cuong, F. Didierjean, G. Duchêne, *et al.*, *Phys. Rev. C* **87**, 054307 (2013).

- [4] R. Li, D. Verney, G. De Gregorio, R. Mancino, I. Matea, L. Coraggio, N. Itaco, M. N. Harakeh, C. Delafosse, F. Didierjean, *et al.*, *Phys. Rev. C* **111**, 034303 (2025).
- [5] L. T. Phuc, N. D. Dang, R. Li, and N. Q. Hung, *Phys. Rev. C* **110**, 064323 (2024).
- [6] P. Hoff and B. Fogelberg, *Nucl. Phys. A* **368**, 210 (1981).
- [7] B. Cheal, J. Billowes, M. L. Bissell, K. Blaum, F. C. Charlwood, K. T. Flanagan, D. H. Forest, S. Fritzsch, C. Geppert, A. Jokinen, *et al.*, *Phys. Rev. C* **82**, 051302 (2010).
- [8] F. H. Garcia, C. Andreoiu, G. C. Ball, A. Bell, A. B. Garnsworthy, F. Nowacki, C. M. Petrache, A. Poves, K. Whitmore, F. A. Ali, *et al.*, *Phys. Rev. Lett.* **125**, 172501 (2020).
- [9] S. Sekal, L. M. Fraile, R. Lica, M. J. G. Borge, W. B. Walters, A. Aprahamian, C. Benchouk, C. Bernards, J. A. Briz, B. Bucher, *et al.*, *Phys. Rev. C* **104**, 024317 (2021).
- [10] F. Ibrahim, D. Verney, M. Lebois, B. Roussiére, S. Essabaa, S. Franchoo, S. Gales, D. G. Mueller, C. Lau, F. Le Blanc, *et al.*, *Nucl. Phys. A* **787**, 110 (2007).
- [11] A. Etilé, D. Verney, N. N. Arsenyev, J. Bettane, I. N. Borzov, M. C. Mhamed, P. V. Cuong, C. Delafosse, F. Didierjean, C. Gaulard, *et al.*, *Phys. Rev. C* **91**, 064317 (2015).
- [12] M. Ciemała, D. Balabanski, M. Csatlós, J. M. Daugas, G. Georgiev, J. Gulyás, M. Kmiecik, A. Krasznahorkay, S. Lalkovski, A. Lefebvre-Schuhl, *et al.*, *Nucl. Instrum. Meth. Phys. Res. Sect. A* **608**, 76 (2009).
- [13] C. Ghosh, V. Nanal, R. G. Pillay, K. V. Anoop, N. Dokania, S. Pal, M. S. Pose, G. Mishra, P. C. Rout, S. Kumar, *et al.*, *J. Instrum.* **11**, P05023 (2016).
- [14] “logft, brookhaven national laboratory, national nuclear data center,” <https://www.nndc.bnl.gov/logft/> (2021).
- [15] R. Li, *First attempt toward a quasi-Pandemonium free β -delayed spectroscopy of ^{80}Ge using PARIS at ALTO*, Thesis, Université Paris-Saclay (2022).
- [16] B. Singh, J. L. Rodriguez, S. S. M. Wong, and J. K. Tuli, *Nuclear Data Sheets* **84**, 487 (1998).
- [17] S. Turkat, X. Mougeot, B. Singh, and K. Zuber, *Atomic Data and Nuclear Data Tables* **152**, 101584 (2023).
- [18] N. Yoshinaga, K. Higashiyama, and P. H. Regan, *Phys. Rev. C* **78**, 044320 (2008).
- [19] “ENSDF, Brookhaven national laboratory, National Nuclear Data Center,” <https://www.nndc.bnl.gov/ensdf/> (2021).
- [20] E. Matthias, E. Recknagel, O. Hashimoto, S. Nagamiya, K. Nakai, T. Yamazaki, and Y. Yamazaki, *Nucl. Phys. A* **237**, 182 (1975).
- [21] A. D. Ayangeakaa, R. V. F. Janssens, C. Y. Wu, J. M. Allmond, J. L. Wood, S. Zhu, M. Albers, S. Almaraz-Calderon, B. Bucher, M. P. Carpenter, *et al.*, *Phys. Lett. B* **754**, 254 (2016).
- [22] A. D. Ayangeakaa, R. V. F. Janssens, S. Zhu, D. Little, J. Henderson, C. Y. Wu, D. J. Hartley, M. Albers, K. Auranen, B. Bucher, *et al.*, *Phys. Rev. Lett.* **123**, 102501 (2019).
- [23] A. M. Forney, W. B. Walters, C. J. Chiara, R. V. F. Janssens, A. D. Ayangeakaa, J. Sethi, J. Harker, M. Alcorta, M. P. Carpenter, G. Gürdal, *et al.*, *Phys. Rev. Lett.* **120**, 212501 (2018).
- [24] J. J. Sun, Z. Shi, X. Q. Li, H. Hua, C. Xu, Q. B. Chen, S. Q. Zhang, C. Y. Song, J. Meng, X. G. Wu, *et al.*, *Phys. Lett. B* **734**, 308 (2014).

* Corresponding author: liren824@gmail.com

† Present address: Faculty of Physics, University of Warsaw, 02-093 Warsaw, Poland.

‡ Present address: University of Novi Sad, Faculty of Science, Novi Sad, Serbia.

[1] M. Wang, W. J. Huang, F. G. Kondev, G. Audi, and S. Naimi, *Chinese Phys. C* **45**, 030003 (2021).

[2] H. Iwasaki, S. Michimasa, M. Niikura, M. Tamaki, N. Aoi, H. Sakurai, S. Shimoura, S. Takeuchi, S. Ota, M. Honma, *et al.*, *Phys. Rev. C* **78**, 021304(R) (2008).

[3] D. Verney, B. Tastet, K. Kolos, F. Le Blanc, F. Ibrahim,